ABSTRACT

Epithelial ovarian cancer (EOC) is one of the most lethal gynaecologic cancers worldwide. Patients often present with late-stage metastatic EOC, characterized by the accumulation of malignant ascites fluid, containing aggregates of cancer cells called spheroids. These patients have a very low survival rate of 30%. As such, there is a huge need to find novel vulnerabilities in metastatic EOC cells that we can exploit for therapeutic benefit, and identify candidate genes which can be targeted to reduce tumour growth and metastasis. Through the use of transcriptome-wide Gene Set Enrichment Analysis (GSEA) of two EOC cell lines (OVCAR8, iOvCa147), we identified various inflammation-associated transcriptional signatures that were enriched in spheroids compared with standard adherent cells. Using nine representative genes, results from RT-qPCR analyses demonstrated that *DEC1*, *TXNIP* and *KLF9* were upregulated in spheroid cells compared to adherent cells across five different EOC cell lines. Using *DEC1,* a transcription factor involved in circadian rhythm, as a candidate gene due to its consistent upregulation across EOC cell lines and expression fold change ranging from a 2.2 to 5.6 increase over adherent cells, siRNA-mediated knockdown experiments were performed to assess whether it has a functional importance in the viability of EOC spheroids. Reducing gene expression of *DEC1* reduced spheroid formation and cell viability in suspension culture as compared to adherent cells where there was no effect. Our identification of novel genes coordinately-regulated and functionally implicated in inflammation responses in EOC spheroids may allow the identification of novel therapeutic targets or biomarkers for early screening in this devastating disease.

INTRODUCTION

Epithelial ovarian cancer (EOC) is known to be the most lethal gynaecological cancer worldwide[1,2]. The high mortality rate and poor 5-year prognosis of EOC patients can be attributed

to its generally non-specific symptoms, and lack of effective early detection methods[2]. Subsequently, patients presenting to clinics often show late-stage metastatic EOC, characterized by the spread of primary tumours to secondary sites within the peritoneal space. Although the 5-year survival rate for individuals with stage I ovarian cancer is >90%, an early stage of detection is more often the exception to the rule. Most patients (75%) present with late-stage (III/IV) ovarian cancer which has a much lower survival rate of 30%[3]. The ovaries are a pair of small organs (2-4cm in diameter) on either side of the uterus, which are not easily accessed by pelvic examination unless they are significantly enlarged[3]. This makes early detection difficult, and signs of the disease are likely to go unnoticed without the use of a more sensitive screening test. When symptoms do present, they are often vague and can be mistaken for gastrointestinal problems or typical post-menopausal symptoms, which further delays the time of detection from the initial clinic visit[3]. It is evident that early detection is essential in preventing the growth and metastases of EOC tumours, especially in asymptomatic individuals where these malignancies may otherwise go unnoticed. Further research is needed in order to identify potential candidate markers for early screening tests, and therapeutic targets to reduce the spread of the disease.

At the point of diagnosis, over one-third of patients present with an accumulation of fluid in the abdominal cavity, called ascites, and this fluid is present in almost all cases of EOC recurrence[4,5]. Malignant ascites fluid promotes a pro-inflammatory and tumorigenic environment, consisting of a mix of tumour cells and stromal cells (such as cytokines, proteins, metabolites and exosomes)[4]. Within the ascites, EOC cells often exist as multi-cellular clusters called spheroids.

Spheroids act as a conduit of metastasis, which attach to the mesothelium and invade the extracellular matrix during dissemination[5]. As EOC cells detach from the primary tumour, they aggregate in the ascites fluid of the peritoneal space to form spheroids prior to implantation and growth in a secondary location. Ascites fluid and the formation of spheroids are defining features of EOC and allow dissemination throughout the pelvic and abdominal regions without the use of the vasculature[6]. This method of anchorage-independent growth suggests that EOC cells are more resistant to anoikis, providing them a survival advantage over single EOC cells[5]. Spheroid cells have also been shown to exhibit more aggressive growth, migration, invasion, and chemo-resistance during favourable conditions *in vitro,* along with the ability to activate survival mechanisms such as an induced state of dormancy during unfavorable conditions[7]. These characteristics make spheroids an elusive target for chemotherapy, and combined with the pro-inflammatory environment of the ascites, foster the acquisition of key cancer hallmarks such as signal-independent proliferation, anti-apoptosis, increased metastasis and chemoresistance[4]. A better understanding of spheroid biology may aid in identifying new therapeutic targets for metastatic EOC and provide an improved prognosis for late-stage EOC patients presenting in the clinic.

Identification of functionally-related gene sets that are coordinately regulated in spheroids can be identified through the use of Gene Set Enrichment Analysis (GSEA) of the transcriptome. Work from our laboratory using two EOC cell lines, OVCAR8 and iOvCa147, demonstrated the presence of nine common transcriptional signatures that are enriched in spheroids compared to standard adherent cells used as a control (Buensuceso & X, unpublished results). These gene expression signatures are of particular interest due to their common regulation in multiple cell

lines, which may suggest these pathways play an important role in spheroid formation in EOC patients. Of these enriched signatures, four are involved in key inflammation-associated pathways, IFN-α, IFN-ɣ, IL-2 and TNF-α. This data provides evidence for a link between the presence of spheroids in EOC patients and the production of pro-inflammatory molecules, both key elements in metastatic ascites which are associated with poor prognosis and reduced quality-of-life for patients[4,8]. The identified genes involved in these potentially dysregulated inflammatory pathways indicate that spheroid cells may induce the production of pro-inflammatory cytokines as found in patients ascites fluid. If disease progression is associated with increased inflammation, then inhibiting downstream targets of these transcriptional pathways and preventing the production of inflammatory molecules may result in better patient prognosis and could prove useful as a therapeutic target for EOC. This leads to my hypothesis that pro-inflammatory pathways become activated in EOC spheroids and promote their metastatic potential.

To test my hypothesis, validation of our previous results generated by the previous GSEA were performed by quantitative RT-PCR analysis of the nine genes coordinately upregulated in spheroid versus adherent cells. Five different cell lines were used to validate these findings; the two cell lines used in our original analysis (iOvCa147, OVCAR8) and three additional EOC cell lines (HeyA8, ES-2, OVCAR-4) to identify patterns of upregulated genes across multiple cell lines. Subsequently, transient RNAi-mediated knockdown of the *DEC1* gene was performed to assess whether it was required for EOC spheroid cell viability. This approach has the overarching goal to reduce EOC spheroid viability through blocking of necessary genes upregulated in spheroid cells. As such, we may identify new therapeutic targets related to inflammation, where drugs

targeting this new upregulated pathway will have increased selectivity to eradicate advanced-stage EOC.

MATERIALS AND METHODS

Cell Culture

OVCAR8 and HeyA8 cell lines were cultured in RPMI-1640 (Wisent). iOvCa147, OVCAR4, and ES-2 cell lines were cultured in DMEM/F12 (Life Technologies). For all cell lines, growth medium was supplemented with 10% fetal bovine serum (FBS). OVCAR8, OVCAR4, ES-2 and HeyA8 cells were obtained from the American Type Culture Collection and iOvCa147 cells were generated previously using malignant ascites derived primary human EOC cells. All cell lines were authenticated by short tandem repeat analysis performed by The Centre for Applied Genomics (The Hospital for Sick Children, Toronto, ON, Canada), and routinely tested for mycoplasma using the Universal Mycoplasma Detection Kit (30-1012K, ATCC). Adherent cells were maintained on tissue-culture-treated polystyrene (Sarstedt). Non-adherent cells were maintained on ultra-low attachment (ULA) cultureware (Corning), which is coated with a hydrophilic, neutrally-charged hydrogel to prevent cell attachment.

RNA Isolation

RNA isolation was performed on each of the five cell lines: HeyA8, OVCAR8, OVCAR4, ES-2 and iOvCa147. For RNA isolation from spheroid cells, cells were seeded at a density of 5×10^5 cells per well of a 6-well ULA cluster plate. Cells were cultured for 1 day in suspension to form spheroids. For adherent cells, cells were seeded at 1×10^6 cells on tissue-culture-treated polystyrene 10 cm dish and cultured for 2 days. Total RNA was isolated from cells grown either

as a monolayer on tissue-culture-treated polystyrene or as spheroids on ULA® cultureware using Qiagen RNeasy Mini Kit (Qiagen). Quantity and quality of purified RNA was determined using a NanoDrop™ One spectrophotometer (NanoDrop Technologies).

Real-time quantitative RT-PCR

Reverse transcription was performed using total RNA isolated from the five EOC cell lines: HeyA8, OVCAR8, OVCAR4, ES-2 and iOvCa147. Reverse transcription was performed using a High-Capacity cDNA Reverse Transcription Kit (Applied Biosystems) based on the manufacturer's protocols. PCR reactions were carried out using Brilliant® SYBR® Green QPCR Master Mix (Agilent Technologies/Stratagene) and the Thermo Fisher QuantStudio™ 3 Real-Time PCR System with data exported to Microsoft® Excel for data analysis. Human specific primers sequences were used to amplify the nine genes of interest: *TXNIP*, *IFIT3*, *HES1*, *KLF9*, *TSC22D1*, *BHLHE40*, *COL6A1*, *NRP1*, and *SMAD3* (**Table 1**). *GAPDH* served as an internal control for cDNA input.

Protein Isolation

Total cellular protein was isolated from adherent and non-adherent EOC cells. Cells were briefly washed twice in ice-cold PBS, dissolved in lysis buffer [50 mM HEPES pH7.4, 150 mM NaCl, 10% glycerol, 1.5 mM $MgCl_2$, 1 mM EGTA, 1 mM sodium orthovanadate, 10 mM sodium pyrophosphate, 10 mM NaF, 1% Triton X-100, 1% sodium deoxycholate, 0.1% SDS, 1 mM PMSF, 1× protease inhibitor cocktail (Roche, Laval, Quebec, Canada)], clarified by centrifugation (20 min at 15,000×*g*), and quantified by Bradford analysis (Bio-Rad Laboratories, Mississauga, Ontario, Canada).

Western Blot

Protein extracts (40 micrograms) were separated by SDS-PAGE using Mini-PROTEAN® TGX™ precast polyacrylamide gels. Proteins were then transferred to a polyvinylidene difluoride membrane (PVDF; Roche, Laval, Quebec, Canada), blocked with 5% skim milk in Tris-buffered saline with Tween-20 (TBST; 10 mM Tris.HCl, pH 8.0, 150 mM NaCl, 0.1% Tween-20). Membranes were washed in TBST and incubated (overnight, 4°C) with the appropriate antibodies in 5% skim milk/TBST. Immunoreactive bands were visualized by incubating (1 h, room temperature) with a peroxidase-conjugated anti-rabbit (1:10,000 in 1% skim milk/TBST; GE Healthcare) followed by exposure to enhanced chemiluminescence reagent (ECL Plus; GE Healthcare). ImageJ software was used to quantify protein band intensities. Antibody against *DEC1 (*NB100-1800SS; 1:15 000) was purchased from Novus Biologicals. Antibodies against vinculin (V9264; 1:20 000) and rabbit IgG (NA934V; 1:10 000) were purchased from Sigma.

siRNA Transfection

Transfections were performed on OVCAR8 cells seeded in 6-well plates using DharmaFECT1 as per manufacturer's protocol (Dharmacon; Thermo Fisher Scientific Inc). si*DEC1* (L-010318-00-0005) and non-targeting control pool #2 (D-001206-14-05) siGENOME SMARTpool siRNA was used. After 72 h, cells were trypsinized, counted, and seeded into either adherent or spheroid conditions. Adherent cells were seeded at a density of 5×10^5 cells per one 10 cm dish for protein isolation and 2 x 10^3 cells per well in a 96-well plate. Cell viability was determined at 72 h post-seeding in 96-well round-bottom ULA cluster plates using CellTiter-Glo® (Promega). Spheroid cells were seeded at a density of 5×10^5 cells per well, in 3-wells of a 6-

well ULA plate for protein isolation and 2×10^3 cells per well in 96-well round-bottom ULA cluster plate. Cell viability was also determined at 72 h post-seeding in 96-well round-bottom ULA cluster plates using CellTiter-Glo® (Promega). Phase-contrast images were captured at 3-hour intervals for a total of 72 hours and confluence was measured using the IncuCyte Zoom imaging platform (Sartorius). Doubling time was determined by fitting an exponential growth curve to the confluence-over-time data (GraphPad Prism 6.05). Phase contrast images were captured of each well containing spheroids using an Olympus IX70 inverted microscope and ImagePro image capture software. The size of each of the spheroids was quantified for each image using the area measurement tool in the *ImageJ* image processing program (NIH).

RESULTS

Elevated RNA expression of inflammation mediators in EOC spheroids

Our lab previously performed a Human Clariom S microarray to screen for transcriptome-wide gene-level variations in gene expression between adherent and spheroid cells using two EOC cell lines, OVCAR8 and iOvCa147. This data was further analyzed using Gene-Set Enrichment Analysis and the Molecular Signatures Datatbase, MSigDB, (Broad Institute) to identify nine upregulated transcriptional pathways in spheroid versus adherent cells common to both the OVCAR8 and iOvCa147 cell lines. Of these pathways, nine candidate inflammation-associated genes were selected for further validation through RT-qPCR. We sought to validate these findings across the two cell lines used in the microarray (OVCAR8, iOvCa147) along with three additional EOC cell lines (HeyA8, OVCAR4, ES-2), to identify any genes consistently upregulated among EOC spheroids. Cells were cultured in either spheroid or adherent conditions and total RNA was collected for subsequent RT-qPCR analysis. The mRNA expression fold-change of all nine genes

were increased in EOC spheroids compared with matched adherent cells in both OVCAR8 and iOvCa147 cell lines (**Fig. 1**). The mRNA levels of the nine genes were largely increased in EOC spheroids of both HeyA8 and ES-2 cells, with the exception of *SMAD3* and *TSC22D1* which were slightly down-regulated in HeyA8 and ES-2 cells, respectively. OVCAR4 exhibited a minimal increase in expression fold-change in spheroid versus adherent cells, and exhibited downregulation of all genes with the exception of *TXNIP*, *KLF9*, and *DEC1*. In fact, these three genes were consistently upregulated across all five EOC cell lines. Of these three, *DEC1* exhibited the most consistent upregulation across EOC cell line spheroids, and biological replicates, with an average expression fold-change ranging from a 2.2 to 5.6-fold increase over adherent cells.

siRNA Knockdown of DEC1 *in OVCAR8 and OVCAR4 cells*

Given that expression of *DEC1* was the most consistently increased inflammation-associated gene in spheroids across all five EOC cell lines, we postulated that this change may be important for the proliferation and survival of EOC spheroids. To examine this further, we planned to test the effect of performing siRNA-mediated knockdowns in two candidate EOC cell lines: OVCAR8 and OVCAR4. This preliminary knockdown assessed whether *DEC1* expression could be reduced in OVCAR8 and OVCAR4 cell lines, using a targeted siRNA (si*DEC1,* L-010318-00-0005) and a non-targeting (siNT) control. The results of the knockdown were quantified by performing a western blot of the total protein lysates collected from adherent cells of both cell lines 72 h post-transfection, using vinculin as a loading control. Subsequent analysis was performed using ImageJ software to quantify protein band intensities (**Fig 2**). In both the OVCAR8 and OVCAR4 cell lines there is a large reduction in *DEC1* expression in cells treated with si*DEC1* compared to the non-targeting siNT control. Protein levels were reduced to 15% and 20% in

OVCAR8 and OVCAR4 cells respectively, compared to the control. This experiment provides evidence for future use of either cell line in spheroid cell viability assays, to demonstrate the effect of reduced *DEC1* expression in spheroid cell survival and proliferation.

siRNA mediated knockdown of DEC1 reduces spheroid cell viability in OVCAR8 cells

Since, we speculate that upregulation of *DEC1* contributes to cell survival in EOC spheroids, we hypothesized that blocking expression through targeted siRNA-mediated knockdowns using *siDEC1* would decrease EOC spheroid cell viability. OVCAR8 cells were transfected with pooled siRNAs against *DEC1* in both adherent and spheroid conditions, and cell viability was quantified using CellTiter-Glo® which measures viability based on the quantification of the ATP present, an indicator of metabolically active cells. Cells in adherent culture were not sensitive to knockdown of *DEC1* with respect to cell viability, as no significant difference in viability was observed between the siNT and si*DEC1* treated cells **(Fig. 3A)**. In contrast, loss of *DEC1* resulted in a reduction in cell viability in spheroids compared to the siNT control, indicating that *DEC1* may promote cell survival and proliferation under the stress of cell detachment as seen in spheroid conditions. Adherent cell confluence and doubling time were measured over 72 h using the IncuCyte Zoom imaging system and subsequent exponential growth curve analysis to generate doubling time measurements (**Fig. 3B and 3D**). No change in percent confluence was observed in adherent cells transfected with either siNT or si*DEC1* providing further evidence in agreement with the CellTiter-Glo® data which suggests that knockdown of *DEC1* in adherent cells does not affect viability. This is also visible in phase contrast images of OVCAR8 adherent cells transfected with either siRNA, which were taken 72 h post transfection, and show no visible difference in

adherent cell size or confluence between the cells treated with si*DEC1* or the siNT control (**Fig 3C**).

As an additional assessment of whether knockdown of *DEC1* decreases spheroid cell viability, spheroid area (in pixels) was quantified from phase contrast images captured at 72 h post transfection after treatment with either si*DEC1* or siNT using ImageJ software (**Fig. 3E and 3F)**. Spheroid cells exhibited a 34% decrease in area, in si*DEC1* transfected spheroid cells as compared with siNT controls. This supports that spheroids lacking *DEC1* are reduced in size, as opposed to only a decrease in ATP production. This is also visible in the phase contrast images of OVCAR8 spheroid cells captured at 72 h post transfection (**Fig. 3F)** where there is an evident decrease in spheroid size between the two conditions, resulting in smaller spheroids when *DEC1* is reduced. These results point to a key role for *DEC1* in maintaining cell viability and proliferation in EOC spheroids, and its upregulation across EOC spheroid cell lines.

DISCUSSION

Inflammation plays a key role in cancer initiation and development, and has been shown to be an important risk factor associated with EOC and patient prognosis[4,9]. Chronic inflammation in EOC patients results in activation of signalling pathways, transcription factors and immune responses, all which contribute to cancer progression and tumorigenesis[4,5,9]. A large contributor to inflammation in EOC is the presence of pro-inflammatory molecules in malignant ascites fluid, which is present in over one-third of patients at the point of diagnosis, and almost all cases of EOC recurrence[4,5,8]. Accumulation of ascites fluid is the result of a combination of factors involving lymphatic obstruction, increased permeability of the vasculature, resident stromal and immune

cells and tumour secretions[8]. In particular, several cytokines such as tumour necrosis factor alpha (TNF-α) and interleukins 2, 6 and 8 (IL-2, IL-6, IL-8) are produced by the tumour itself or activated by nearby immune cells[10]. Higher serum and ascites levels of these cytokines have been found in patients with EOC than in patients with other malignancies, and correlate with the severity of the disease and poor clinical outcomes[9, 10, 11]. In addition to the accumulation of ascites, the formation of spheroids within the ascites fluid of the peritoneal space is a defining feature of EOC, and spheroids represent the primary conduit of EOC metastasis[6]. For this reason, understanding the mechanisms responsible for tumour-promoting inflammation, and how spheroid cells may promote the production of pro-inflammatory molecules is crucial in understanding EOC progression, and to identify targets to reduce the proliferation and metastasis of EOC tumours.

Our lab generated new preliminary evidence that there are several inflammation-associated transcriptional signatures coordinately upregulated in spheroid versus adherent cells in two EOC cell lines, OVCAR8 and iOvCa147 (Buensuceso & X, unpublished results). These signatures include both the TNF-α and IL-2 signaling pathways, providing evidence for a link between the formation of spheroids in EOC patients, and the production of pro-inflammatory molecules. Using nine candidate genes involved in inflammatory pathways and upregulated in both OVCAR8 and iOvCa147 spheroids, we validated these findings among previously-tested EOC cell lines, and three additional cell lines: HeyA8, OVCAR4 and ES-2. RT-qPCR analysis showed that all nine candidate genes were upregulated across OVCAR8 and iOvCa147 spheroids, with three genes being upregulated across all five EOC spheroid cell lines (*TXNIP, KLF9,* and *DEC1*). We chose *DEC1* as a candidate gene for subsequent siRNA-mediated knockdown experiments due to its consistent upregulation across all cell lines, and high expression fold change ranging from a 2.2-

5.6 fold increase over adherent cells. Knockdown of *DEC1* resulted in a decrease in spheroid cell viability and growth over the course of the 72 h culture period, compared to adherent cells. This was quantified using both a CellTiter-Glo® assay to indirectly measures viability based on the quantification of the ATP present, an indicator of metabolically active cells, and spheroid area in pixels, which was quantified using phase contrast images captured 72 h post-seeding and ImageJ software. Since the CellTiter-Glo® assay only infers cell viability from the relative ATP present, the inclusion of the spheroid size measurements substantiates this result since there is a reduction in spheroid size indicating fewer viable cells. This data supports our claim that pro-inflammatory pathways become activated in EOC spheroids and promote their metastatic potential; this takes us one step closer to achieving our goal of reducing spheroid viability through blocking necessary genes upregulated in spheroid cells, which may be involved in essential cellular pathways during metastasis.

These findings are consistent with the available literature which suggests that *DEC1* has a role in tumour progression and malignant potential of various cancers such as invasive breast cancers, non-small cell lung carcinoma, and hepatocellular carcinoma[12-16]. Differentiated embryo-chondrocyte expressed gene 1, *DEC1*, is a basic helix-loop-helix transcription factor involved in a wide range of cellular processes involving hypoxia-driven epithelial to mesenchymal transition (EMT), p53-mediated reversible cell quiescence, and circadian rhythm[16, 17, 18]. In the context of inflammation, *DEC1* expression is induced by TNF-α, a common inflammatory pathway upregulated in EOC patient ascites fluid[20]. Elevated TNF-α levels in patient ascites samples is also associated with reduced progression-free survival (PFS), suggesting that elevated *DEC1*

expression may be correlated with poor patient prognosis and could be used to evaluate PFS in patients presenting with EOC in the clinic[10].

Previous research has studied the role of *DEC1* in hepatocellular carcinoma, where it is induced under hypoxic conditions and negatively regulates both hypoxia-inducible factor alpha (HIF-α) and E-cadherin[16]. This change in gene expression promotes EMT in tumour cells, an important hallmark of metastasis. In fact, our group has documented the induction of EMT in EOC spheroids[21]. This phenomenon is also evident in breast carcinoma, where the overexpression of *DEC1* in breast cancer correlates with the reduction of claudin-1, a gene responsible for the maintenance of tight junctions between cells. Downregulation of claudin-1 is ultimately involved in tumorigenesis of multiple cancer types involving breast, prostate and melanoma, and promotes EMT by reducing cell-to-cell adhesions[13].

In colon carcinoma, research into *DEC1* upregulation has focused on its role in p53-mediated quiescence and how expression of this gene is induced via DNA damage in a p53-dependent manner resulting in reduced cell proliferation[18,19]. The induction of quiescence in fibroblast cells induces nuclear atypia in neighboring epithelial cells of EOC spheroids and shows that it may be involved in the process of neoplastic transformation[24]. *DEC1* overexpression results in decreased cyclin D1, which promotes transition from G_1 to S phase, providing evidence that *DEC1* upregulation may induce cellular quiescence[23]. Our group has previously demonstrated that EOC spheroids undergo a dormancy phenotype by inducing cellular quiescence, that is reversible upon spheroid re-attachment[22].

It is unsurprising, due to the diverse role of *DEC1* in cell function, that it would be implicated in spheroid cell formation and be especially relevant in the context of EOC. Spheroid cells are known to show more aggressive growth, migration and invasion and survive under a variety of environmental stressors[7]. Upregulation of *DEC1* may act as a survival response by spheroids to induce a state of reversible quiescence, in order to survive detachment from the primary lesion and survive for prolonged periods of time in the peritoneal space prior to reattachment at a secondary location. Quiescence may also represent a mechanism where tumour cells can evade the toxicity of chemotherapy and radiation, to allow the eventual re-emergence from cell cycle arrest and facilitate disease recurrence from a dormant state. The ability of *DEC1* to promote EMT may also provide a benefit to spheroid cells, and allow them to take on a mesenchymal phenotype, allowing detachment from the epithelium and suspension in culture. The induction of *DEC1* under hypoxic conditions is especially relevant, since oxygen levels are commonly decreased in malignant ascites, creating a hypoxic environment. Induction of *DEC1* may act as a protective mechanism against hypoxia-induced cell death, allowing spheroids to survive in environments with little oxygen[25].

What is surprising is the implication of circadian rhythm in EOC spheroid formation which has not previously been studied. *DEC1* is implicated in circardian rhythm and suppresses CLOCK/BMAL-1 promoter activity with overexpression of *DEC1* delaying the phase of clock genes such as *Dec1, Dec2, Per1, and Dbp.* The loss of *DEC1*, modelled in a *DEC1*$^{-/-}$ mouse, demonstrated this, and resulted in longer circadian periods[17]. Activation of genes downstream of *DEC1* such as *Per1* has been implicated in certain cancers but its role as an activator or suppressor of apoptosis is still unclear[14]. What is clear is that the biological functions of *DEC1*, such as

facilitating cell proliferation and EMT, is regulated through circadian rhythms, and that this gene mediates crosstalk between circadian rhythm and physiological actions[14]. This suggests that tumor cell malignancy may also be regulated by circadian rhythm. Studies have shown that the disturbance of circadian rhythm may be linked to cancer, as night work has been shown to increase cancer risk and excessive daytime sleepiness is associated in children with a high incidence of cancer[14,26]. More research is needed to elucidate the role of circadian rhythm in EOC by analyzing the regulation of other relevant genes. If upregulation of circadian rhythm associated genes is indeed associated with EOC spheroid formation this would suggest the potential therapeutic benefit of chronotherapy. Chronotherapy, where anti-cancer drugs are administered at optimal times according to circadian rhythm, has been useful when treating with anti-tumour drugs to reduce cytotoxicity and increase effectiveness in patients[14]. Previous research has shown success in treating patients with 5-fluorouracil using chronotherapy, as determined through computational modelling[27]. This would provide a means to improve current EOC treatment by optimizing the administration of currently approved drugs, in accordance with EOC cell circadian rhythms.

Limitations to these findings include the lack of western blot data to assess the efficacy of *DEC1* knockdown in OVCAR8 cells, increasing biological replicates during cell viability experiments, and using more direct measurements of cell viability for future studies. Although preliminary western blot analyses were conducted to assess the efficacy of siRNA mediated *DEC1* knockdown in both OVCAR8 and OVCAR4 cells (**Fig. 2**) this was not repeated in the subsequent siRNA-mediated knockdown experiment in OVCAR8 cells. Therefore, we cannot be certain that the knockdown was effective in the OVCAR8 spheroids, and the observed reduction in viability and spheroid size could be due to other confounding factors. To increase the credibility of the cell

viability assay data, further biological replicates should be used to generate more significant data regarding the reduced viability of OVCAR8 spheroids. Repeating the procedure in the other EOC cell lines (OVCAR4, iOvCa147, HeyA8, ES-2) would also assess whether these finding are consistent across EOC spheroids, similar to how the upregulation of *DEC1* was observed across all five cell lines. Finally, since CellTiter-Glo® is an indirect measurement of cell viability, that uses ATP levels as a proxy for viable cells, future studies could use trypan blue exclusion assays to quantify cell viability directly. This assay is a measurement of the proportion of live to dead cells within a sample, and a more accurate representation of cell viability.

Future research should not be limited to the study of *DEC1* in spheroid formation, and should also assess the functional importance of the other inflammation-associated genes upregulated in spheroids, on cell viability and proliferation. Genes *TXNIP* and *KLF9* are both candidates for future cell viability assays based on their upregulation across all five EOC lines and previous research linking their expression to cancer growth and metastasis[28, 29]. Whereas *DEC1* and *KLF9* overexpression is shown to be oncogenic in terms of tumour growth, *TXNIP* has been previously characterized as a tumour suppressor gene[28]. This suggests that the association between inflammation and EOC spheroid formation is a complex process involving the combined effects of multiple genes which evoke positive or negative effects on spheroid growth and formation. Improving our understanding of the key inflammatory pathways implicated in spheroid formation, and the genes essential to spheroid viability allows a more complete understanding of the role of the tumour microenvironment in EOC progression. Further research into the role of inflammation in EOC spheroids may result in the identification of novel therapeutic targets for treatment,

markers for poorer prognosis, such as *DEC1*, or result in improvements to current dosage regimens, such as optimizing treatment based on the inherent circadian rhythms of cancer cells.

References

1. Chang, L. C., Huang, C. F., Lai, M. S., Shen, L. J., Wu, F. L., and Cheng, W. F. (2018). Prognostic factors in epithelial ovarian cancer: A population-based study. PloS one, *13*(3), e0194993. doi:10.1371/journal.pone.0194993

2. Motohara, T., Masuda, K., Morotti, M., Zheng, Y., El-Sahhar, S., Chong, K. Y., *et al*. (2019). An evolving story of the metastatic voyage of ovarian cancer cells: cellular and molecular orchestration of the adipose-rich metastatic microenvironment. Oncogene, *38*(16), 2885–2898. doi:10.1038/s41388-018-0637-x

3. Karst, A. M., and Drapkin, R. (2009). Ovarian Cancer Pathogenesis: A Model in Evolution. Journal of Oncology, *2010,* Article 932371. doi:10.1155/2010/932371

4. Kim, S., Kim, B., & Song, Y. S. (2016). Ascites modulates cancer cell behavior, contributing to tumor heterogeneity in ovarian cancer. Cancer science, *107*(9), 1173–1178. doi:10.1111/cas.12987

5. Al Habyan, S., Kalos, C., Szymborski, J. and McCaffrey, L. (2018). Multicellular detachment generates metastatic spheroids during intra-abdominal dissemination in epithelial ovarian cancer. Oncogene, *37,* 5127–5135 doi:10.1038/s41388-018-0317-x

6. Shield, K., Acklad, M. L., Ahmed, N., and Rice, G. E. (2009). Multicellular spheroids in ovarian cancer metastases: Biology and pathology. Gynecologic Oncology, *113*(1), 143-148. doi: https://doi.org/10.1016/j.ygyno.2008.11.032

7. Liao, J., Qian, F., Tchabo, N., Mhawech-Fauceglia, P., Beck, A., Qian, Z., *et al*. (2014). Ovarian cancer spheroid cells with stem cell-like properties contribute to tumor generation, metastasis and chemotherapy resistance through hypoxia-resistant metabolism. PloS one, *9*(1), e84941. doi:10.1371/journal.pone.0084941

8. Ahmed, N., and Stenvers, K. L. (2013). Getting to know ovarian cancer ascites: opportunities for targeted therapy-based translational research. Frontiers in Oncology, *3*, 256. doi:10.3389/fonc.2013.00256

9. Savant, S. S., Sriramkumar, S., and O'Hagan, H. M. (2018). The Role of Inflammation and Inflammatory Mediators in the Development, Progression, Metastasis, and Chemoresistance of Epithelial Ovarian Cancer. Cancers, *10*, 251. doi:10.3390/cancers10080251

10. Chon, H. S., Sehovic, M., Marchion, D., Walko, C., Xiong, Y., and Extermann, M. (2019). Biologic Mechanisms Linked to Prognosis in Ovarian Cancer that May Be Affected by Aging. Journal of Cancer, *10*(12), 2604-2618. doi:10.7150/jca.29611

11. Dobrzycka, B., Terlikowski, S. J., Kowalczuk, O., and Kinalski, M. (2009). Circulating Levels of TNF-alpha and Its Soluble Receptors in the Plasma of Patients With Epithelial Ovarian Cancer. European cytokine network, *20*(3), 131-134. doi:10.1684/ecn.2009.0161

12. Chakrabarti, J., Turley, H., Campo, L., Han, C., Harris, A. L., Gatter, K. C., and Fox, S. B. (2004). The transcription factor DEC1 (stra13, SHARP2) is associated with the hypoxic response and high tumour grade in human breast cancers. British Journal of Cancer, *91*, 954-958. doi: https://doi.org/10.1038/sj.bjc.6602059

13. Liu, Y., Miao, Y., Wang, J., Lin, X., Wang, L., Xu, H., and Wang, E. (2013). DEC1 is positively associated with the malignant phenotype of invasive breast cancers and negatively correlated with the expression of claudin-1. International Journal of Molecular Medicine, *31*, 855-860. doi: https://doi.org/10.3892/ijmm.2013.1279

14. Sato, F., Bhawal, U. K., Yoshimura, T., and Muragaki, Y. (2016). DEC1 and DEC2 Crosstalk between Circadian Rhythm and Tumor Progression. Journal of Cancer, *7*(2), 153-159. doi: 10.7150/jca.13748

15. Liu, Y., Wang, L., Lin, X., Wang, J., Yu, J., Miao, Y., and Wang, E. (2013). The transcription factor DEC1 (BHLHE40/STRA13/SHARP-2) is negatively associated with TNM stage in non-small-cell lung cancer and inhibits the proliferation through cyclin D1 in A549 and BE1 cells. Tumor Biology, *34*, 1641-1650. doi: https://doi.org/10.1007/s13277-013-0697-z

16. Murakami, K., Wu, Y., Imaizumi, T., Aoki, Y., Liu, Q., Yan, X., *et al*. (2017). DEC1 Promotes Hypoxia-Induced Epithelial-Mesenchymal Transition (EMT) in Human Hepatocellular Carcinoma Cells. Biomedical Research Foundation, *38*(4), 221-227. doi: 10.2220/biomedres.38.221

17. Nakashima, A., Kawamoto, T., Honda, K. K., Ueshima, T., Noshiro, M., Iwata, T., *et al*. (2008). DEC1 Modulates the Circadian Phase of Clock Gene Expression. Molecular and Cellular Biology, *28*(12), 4080-4092. doi: 10.1128/MCB.02168-07

18. Qian, Y., Zhang, J., Yan, B., and Chen, X. (2008). DEC1, a Basic Helix-Loop-Helix Transcription Factor and a Novel Target Gene of the p53 Family, Mediates p53-dependent Premature Senescence. The Journal of Biological Chemistry, *283*, 2896-2905. doi: 10.1074/jbc.M708624200

19. Li, Y., Zhang, H., Xie, M., Hu, M., Ge, S., Yang, D., *et al*. (2002). Abundant Expression of Dec1/stra13/sharp2 in Colon Carcinoma: Its Antagonizing Role in Serum Deprivation-Induced Apoptosis and Selective Inhibition of Procaspase Activation. The Biochemical Journal, *367*(Pt. 2), 413-422. doi: 10.1042/BJ20020514

20. Liu, Y., Sato, F., Kawamoto,T., Fujimoto, K., Morohashi, S., Akasake, H., *et al*. (2010). Anti-apoptotic effect of the basic helix-loop-helix (bHLH) transcription factor DEC2 in human breast cancer cells. Genes to Cells, *15*(4), 315-325. doi: 10.1111/j.1365-2443.2010.01381.x

21. Rafehi, S. (2016). Exploring the regulation and function of epithelial-mesenchymal plasticity in ovarian cancer spheroids. Electronic Thesis and Dissertation Repository, 3706. doi: https://ir.lib.uwo.ca/etd/3706

22. Correa, R. J. M., Peart, T., Valdes, Y. R., DiMattia, G. E., and Shepherd, T. G. (2012). Modulation of AKT activity is associated with reversible dormancy in ascites-derived epithelial ovarian cancer spheroids. Carcinogenesis, *33*(1), 49-58. doi: https://doi.org/10.1093/carcin/bgr241

23. Bhawal, U. K., Sato, F., Arakawa, Y., Fujimoto, K., Kawamoto, T., Tanimoto, K. (2011). Basic Helix-Loop-Helix Transcription Factor DEC1 Negatively Regulates Cyclin D1. Journal of Pathology, *224*(3), 420-429. doi: 10.1002/path.2878

24. Lawrenson, K., Grun, B., Benjamin, E., Jacobs, I. J., Dafou, D., and Gayther, S. A. (2010). Senescent Fibroblasts Promote Neoplastic Transformation of Partially Transformed Ovarian Epithelial Cells in a Three-dimensional Model of Early Stage Ovarian Cancer. Neoplasia, *12*(4), 317-325. doi: 10.1593/neo.91948

25. Huang, H., Li, Y., Liu, J., Zheng, M., Feng, Y., Hu, K., *et al*. (2012). Screening and Identification of Biomarkers in Ascites Related to Intrinsic Chemoresistance of Serous Epithelial Ovarian Cancers. PLos One, *7*(12), e51256. doi: 10.1371/journal.pone.0051256

26. Parent, M. E., El-Zein, M., Rousseau, M. C., Pintos, J., and Siemiatycki, J. (2012). Night Work and the Risk of Cancer Among Men. American Journal of Epidemiology, *176*(9), 751-759. doi: 10.1093/aje/kws318

27. Altinok, A., Lévi, F., and Goldbeter, A. (2009). Identifying Mechanisms of Chronotolerance and Chronoefficacy for the Anticancer Drugs 5-fluorouracil and Oxaliplatin by Computational Modeling. European Journal of Pharmaceutical Sciences, *36*(1), 20-38. doi: 10.1016/j.ejps.2008.10.024

28. Spaeth-Cook, D., Burch, M., Belton, R., Demoret, B., Grosenbacher, N., David, J., *et al*. (2018). Loss of TXNIP enhances peritoneal metastasis and can be abrogated by dual TORC1/2 inhibition. Oncotarget, *9*(86), 35676-35686. doi: 10.18632/oncotarget.26281

29. Zhang, Q., Dou, H., Tang, Y., Su, S., and Lieu, P. (2015). Lentivirus-mediated knockdown of Krüppel-like factor 9 inhibits the growth of ovarian cancer. Archives of Gynecology and Obstetrics, *291*, 377-382. doi: https://doi-org.proxy1.lib.uwo.ca/10.1007/s00404-014-3405-3

FIGURES

Gene	Forward Primer Sequence	Reverse Primer Sequence
TXNIP	CAGCAGTGCAAACAGACTTCGG	CTGAGGAAGCTCAAAGCCGAAC
IFIT3	CCTGGAATGCTTACGGCAAGCT	GAGCATCTGAGAGTCTGCCCAA
HES1	GGAAATGACAGTGAAGCACCTCC	GAAGCGGGTCACCTCGTTCATG
KLF9	CTACAGTGGCTGTGGGAAAGTC	CTCGTCTGAGCGGGAGAACTTT
TSC22D1	CTCTGGTGCAAGTGTGGTAGCT	ACCTCCACTTCTTCTCTGACCG
SMAD3	TGAGGCTGTCTACCAGTTGACC	GTGAGGACCTTGTCAAGCCACT
DEC1	TAAAGCGGAGCGAGGACAGCAA	GATGTTCGGGTAGGAGATCCTTC
COL6A1	GCCTTCCTGAAGAATGTCACCG	TCCAGCAGGATGGTGATGTCAG
NRP1	AACAACGGCTCGGACTGGAAGA	GGTAGATCCTGATGAATCGCGTG

Table 1: Forward and reverse PCR primer sequences used for RT-qPCR analyses of *TXNIP, IFIT3, KLF9, HES1, DEC1, TSC22D1, SMAD3, NRP1* and *COL6A1*

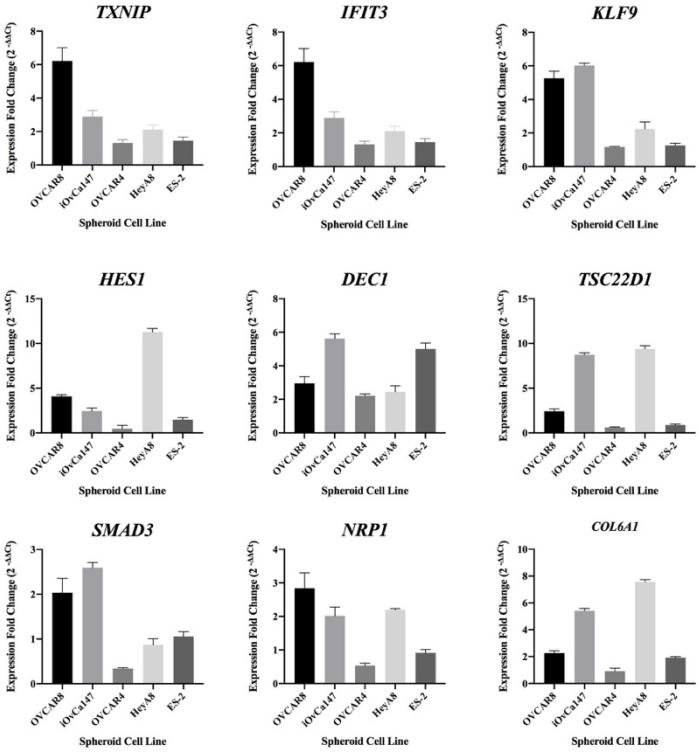

Figure 1: Inflammation-associated genes are upregulated in spheroids across EOC cell lines. Quantitative RT-PCR analysis of *TXNIP, IFIT3, KLF9, HES1, DEC1, TSC22D1, SMAD3, NRP1* and *COL6A1* cDNA in monolayer/spheroid cells. RNA was isolated from adherent and spheroid cells at 48 h and 24 h post-seeding in five EOC cell lines, OVCAR8, iOvCa147, OVCAR4, HeyA8 and ES-2. Expression fold-change ($2^{-\Delta\Delta Ct}$) was quantified against GAPDH as an internal control, and the monolayer culture as the untreated condition. Data is represented as mean ± SEM, with a n=3.

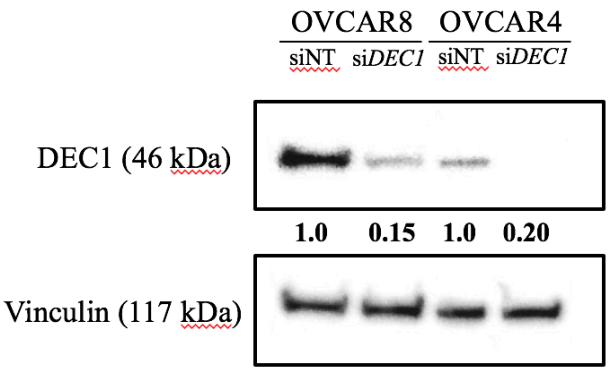

Figure 2: Western blot analysis of si*DEC1* and siNT control in adherent OVCAR8 and OVCAR4 cells. Cells were grown in adherent culture and treated with either si*DEC1* or a non-targeting siNT control. Protein lysates were collected at 72 hours, and western blot analysis was performed to detect the presence of *DEC1,* vinculin was used as a loading control. Densitometric analysis was performed to quantify *DEC1* expression relative to vinculin.

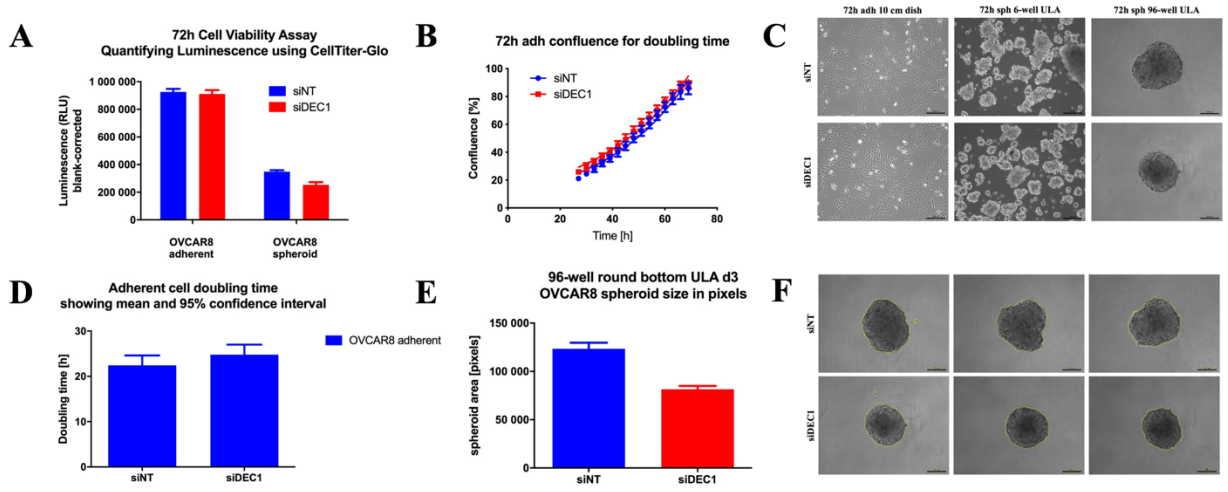

Figure 3: Inhibition of DEC1 reduces spheroid viability in OVCAR8 cells in vitro. (A) OVCAR8 cells were transfected with either si*DEC1* or a siNT control and grown in culture for 72 h. Cells then were seeded into either adherent or spheroid conditions in 96-well adherent or ULA plates respectively at a density of 2 x 10^3 cells per well. Cell viability was determined after 72 h using CellTiter-Glo®assay to quantify luminescence which is proportional to the amount of ATP present, as a measure of metabolically active cells. Data is represented as mean ± SEM. **(B)** % confluence for OVCAR8 cells grown in adherent culture conditions and treated with either siDEC1 or siNT. Confluence was monitored over 3 days using the IncuCyte Zoom imaging system. Data is represented as mean ± SEM. **(C)** Phase contrast images of OVCAR8 adherent and spheroid cells treated with either siDEC1 or siNT. Images taken at 72 h post transfection on 10 cm polystyrene dish, 72 h post-transfection on 6-well ULA plates, or spheroids 72 hours post seeding for CellTiter-Glo® assay in 96-well ULA plate. Scale bars represent 200 µm. **(D)** Doubling time for OVCAR8

cells grown in adherent culture conditions and treated with either si*DEC1* or siNT. Phase-contrast images were captured at 3-hour intervals for a total of 72 hours and confluence was measured using the IncuCyte Zoom imaging platform. Doubling time was determined using GraphPad Prism 6.0 by fitting an exponential growth curve to confluence over time data. Data is represented as mean ± SEM. **(E)** Spheroid area (in pixels) was quantified from phase contrast images (F) with ImageJ software from spheroid cells treated with si*DEC1* or siNT. Data is represented as mean ± SEM. **(F)** Phase contrast images of OVCAR8 spheroid cells captured at 72 h post transfection after treatment with either si*DEC1* or siNT. Images taken of 96-well ULA plate using an Olympus IX70 inverted microscope and ImagePro image capture software.. Scale bars represent 200 μm.